Feshbach resonances and limiting universal thermodynamics of strongly correlated nucleons

A. Z. Mekjian

Department of Physics and Astronomy, Rutgers University, Piscataway, New Jersey 08854, USA

A finite-temperature model of strongly correlated nucleons with underlying isospin symmetries is developed. The model can be used to study the role of bound states and Feshbach resonances on the thermal properties of a spin 1/2, isospin 1/2 system of protons and neutrons by varying the proton fraction. An analysis of features associated with a universal thermodynamic limit or unitary limit is given. In the limit of very large scattering length, the effective range to quantum thermal wavelength appears as a limiting scale in an interaction energy and equation of state.

The behavior of dilute Fermi systems is of recent interest in both atomic systems and in nuclear systems. Early theoretical interest arose when Bertsch [1] formulated a many-body challenge problem for systems with large scattering length compared to interparticle spacings. This regime is referred to as the unitary limit. Experimental studies of cold gases in the unitary regime in atomic physics were carried out by several groups [2–5]. In atomic systems Feshbach resonances have provided a unique tool for studies of such systems. In particular, tuning across a Feshbach resonance via a magnetic field has been a very successful method in the study of the transition from a Bose-Einstein condensate of tightly bound dimers to a Bardeen Schrieffer Cooper (BSC) superfluid state. Some early theoretical studies of atomic systems were carried out by Ho and collaborators both at $T = 0$ [6] and $T \neq 0$ [7]. Moreover, the results in Ref. [7] showed that several of the features of a degenerate $T = 0$ Fermi gas are present in the high-temperature Boltzmann limit. In nuclear physics, a Monte Carlo investigation of the superfluid properties of a system of pure neutrons was done in Ref. [8]. Further theoretical understanding of the pure neutron system came from the extensive work of Bulgac and collaborators (see Ref. [9] and references therein and Ref. [10]). Early work on the Bertsch problem was done by Barker [10] and Heiselberg [11]. The equation of state of neutron matter [12] and nuclear matter [13] using nonperturbative lattice methods has also been developed. The results in Ref. [13] showed a sharp transition from an uncorrelated Fermi gas to a clustered system. The inner crust of a neutron star is an example where dilute Fermi gases occur [14]. References [15–18] contain discussions of the virial expansion approach to nondegenerate Fermi systems, which forms the basis of the present work. Recursive methods to obtain the nuclear canonical partition function in a cluster-virial expansion [19] have also been developed and used to study nuclear liquid-gas phase transitions [20,21].

The focus of this paper centers around thermodynamic properties of strongly correlated fermions and in particular to a two-component hadronic system made of protons and neutrons, each with two spin states and underlying isospin symmetries. Real hadronic systems contain both neutrons and protons even in the limit of neutron stars, which contain a small fraction of protons. Moreover, future FRIB (Facility for Rare Isotope Beams) experiments will study properties of nuclei with large neutron and proton excess. An investigation of a two-component system is a rich extension of results from a one-component system. For example, in a system of protons and neutrons both isospin symmetries and features associated with spin structure come into play. The np system has a bound state in the spin $S = 1$, isospin $I = 0$ state, whereas the nn $S = 0$, $I = 1$ system and np $S = 0$, $I = 1$ system have resonant-like virtual states with very large scattering lengths. Also, the formation of deuterons in a dilute Fermi system [15] is a precursor to the liquid-gas phase transition [20,21]. In a liquid-gas phase transition clusters of all sizes appear. The specific heat shows a singular behavior around the first-order liquid-gas phase transition [21]. The nuclear system does not allow tuning with a magnetic field nor having the feature of an infinite scattering length as in atomic systems. However, variations of the proton fraction changes the scattering length from a large negative number for pure neutrons to a system where bound-np deuterons and higher clusters are also present as the proton fraction is increased. Temperature also plays an important part in the number of bound and virtual states as does the proton fraction y.

The equation of state (EOS) around a nondegenerate limit has a virial expansion that is $PV/k_B T = A - (x_2/x_1^2) A^2 + [(4x_2^2 - 2x_1 x_3)/x_1^4] A^3 + [(-20x_2^3 + 18x_1 x_2 x_3 - 3x_1^2 x_4)/x_1^6]A^4 \cdots$ with x_k correlation or cluster coefficients. For a one-component system of identical fermions, antisymmetrization effects result in $x_k = (-1)^{k+1}/k^{5/2}(V/\lambda_T^3)$. The thermal wavelength is $\lambda_T = h/\sqrt{2\pi m k_B T}$. A virial expansion is valid when $(A/V)\lambda_T^3$ is small. These results can be extended to include interactions by considering the following model with two components made of protons and neutrons. The pressure in a dilute interacting gas to second order in the density is $PV/k_B T = A - b_2 A^2$, where the coefficient $b_2 \sim 1/V$ has contributions from nn, pp, and np components. To see the structure of b_2 a simple example will be given where all three systems can form an s-wave bound state, with the np system having two possibilities with spin $S = 1$, the deuteron, or $S = 0$. This will then be corrected for continuum interactions and the nn and pp bound states will be turned off. The law of partial pressures leads to a total pressure $PV/k_B T = N_p + N_n + N_{nn} + N_{pp} + N_{np}$, with $Z = N_p + N_{np} + 2N_{pp}$, $N = N_n + N_{np} + 2N_{nn}$, and

$A = Z + N$. The number of particles $N_{ij}(S)$ as a function of spin S

$$N_{ij}(S) = \frac{2S+1}{2^2} 2^{3/2} \frac{\lambda_T^3}{V} \exp\left[\frac{E_B(ij,S)}{k_B T}\right] N_i N_j Z$$
$$\equiv a_2(ij,S) N_i N_j, \tag{1}$$

with $i = p, n$ and $j = p, n$. This law expresses chemical equilibrium [15]. $N_{ij}(S)$ is strongly T dependent with higher T breaking the bound state into its constituents. $E_B(ij)$ equals the binding energy of the pair. Writing $N_p = Z - N_{np} - 2N_{pp}$, $N_n = N - N_{np} - 2N_{nn}$, proton fraction $y_p = y = Z/A$, and neutron fraction $y_n = N/A = 1 - y_p = 1 - y$ leads to an EOS to order A^2 that is

$$\frac{PV}{k_B T} = A + \frac{1}{2^{5/2}} \frac{\lambda_T^3}{(2S+1)V}[y^2 + (1-y)^2]A^2$$
$$- \sum_S \sum_{i\&j=p,n} y_i y_j a_2(ij,S) A^2. \tag{2}$$

Antisymmetrization corrections in the pp and nn channels are included in this equation. As noted the pp, nn, and np $S = 0$, $I = 1$ channels have no bound states. However, a resonance-like virtual state acts as a bound state and makes a contribution to the A^2 term through a term due to Beth and Ulhenbeck [22–24] that changes the bound-state Boltzmann factor to a continuum correlation integral. Specifically, $\exp[E_B/k_B T] \rightarrow (1/\pi) \int (\partial \delta_0/\partial k) \exp(-\hbar^2 k^2/2\mu k_B T) dk$, where δ_0 is the s-wave phase shift and $\mu = m/2$ is the reduced mass. Higher orbital l correlations can also contribute using $\partial \delta_0/\partial k \rightarrow \Sigma_l (2l+1) d\delta_l/dk$. Here only s waves will be considered in detail but some features associated with higher partial waves will also be mentioned.

The volume dependence of the energy can be obtained from $\partial E/\partial V)_T = T \partial P/\partial T)_V - P$. For $P = k_B T(A/V - \hat{b}_2 A^2/V^2)$ with $\hat{b}_2/V = b_2$ the volume dependence of the energy is $E(V) = T(\partial \hat{b}_2/\partial T) k_B T(A^2/V)$, where

$$\hat{b}_2 = -\frac{\lambda_T^3}{2^{7/2}}[y^2 + (1-y)^2]Z$$
$$+ \sum_S \sum_{i\&j=p,n} y_i y_j \frac{2S+1}{2^2} 2^{3/2} \lambda_T^3 \left[\sum_B \exp\left(\frac{E_B(ij,S)}{k_B T}\right)\right.$$
$$\left. + \frac{1}{\pi} \int \frac{\partial \delta_0(ij,S)}{\partial k} \exp(-\hbar^2 k^2/mk_B T) dk Z\right]$$
$$\equiv \hat{b}_{2,\text{sym}} + \hat{b}_{2,\text{int}}. \tag{3}$$

This volume dependence comes from antisymmetrization (the term involving $1/2^{7/2}$ or $\hat{b}_{2,\text{sym}}$) and from interaction terms (terms with E_B, $\partial \delta_0/\partial k$, or $\hat{b}_{2,\text{int}}$) with the latter called interaction energy. The interaction energy density is

$$\varepsilon_{\text{int}} = \frac{E_{\text{int}}}{V} = \frac{3}{2} k_B T \frac{A^2}{V^2} \lambda_T^3 \sum_S \sum_{i\&j=p,n} y_i y_j \frac{2S+1}{2^2} 2^{3/2}$$
$$\times \left(-B_{B,C}(ij,S) + \frac{2}{3} T \frac{\partial B_{B,C}(ij,S)}{\partial T}\right), \tag{4}$$

where $B_{B,C}(ij,S) = B_B(ij,S) + B_C(ij,S)$ with

$$B_B(ij,S) = \sum_B \exp\left(\frac{E_B(ij,S)}{k_B T}\right),$$
$$B_C(ij,S) = \frac{1}{\pi} \int \frac{\partial \delta_0(ij,S)}{\partial k} \exp(-\hbar^2 k^2/mk_B T) dk. \tag{5}$$

A rescaled energy density is defined as $\hat{\varepsilon}_{\text{int}} \equiv \varepsilon_{\text{int}}/[(3k_B T/2) (A/V)^2 \lambda_T^3 2^{3/2}/4]$. The experimental determination of the interaction energy in the unitary limit in atomic systems can be found in Refs. [2,3] and a calculation of it is in Ref. [7] at nonzero T. At $T = 0$, a numerical coefficient ξ relating the energy in the unitary limit to the noninteracting Fermi gas energy is of interest. Specifically, $E/N = \xi(3E_F/5)$, where $\xi \approx 0.3$–0.4 [8,11].

The nuclear force has a short-range repulsive part besides an attractive longer range part. A simplified interaction with an infinite repulsive core for $0 \leqslant r \leqslant c$ and an attractive square well of depth V_0 for $c \leqslant r \leqslant R$ has $\delta_0 = \arctan[(k/\alpha)\tan(\alpha(R-c))] - k(R-c) - kc$, with $\alpha^2 = k^2 + \alpha_0^2$ and $\alpha_0 = \sqrt{2\mu V_0/\hbar^2}$. When the square well has no bound state then $\delta_o = 0$ at $k = 0$ and reaches a maximum value $\delta_{0,m} = \pi/2 - \sqrt{\pi^2/4 - (2\mu V_0 \hat{R}^2/\hbar^2)}$ at $k\hat{R} = k_m \hat{R} = \pi/2 - \delta_{0,m}$, $\hat{R} = R - c$. For a well with a single bound state $\delta_o = \pi$ at $k = 0$. When $k \ll \alpha_0$ the behavior of the phase shift is given by an effective range theory, which reads $k \cot \delta_0 = -(1/a_{\text{sl}}) + r_0 k^2/2$. The scattering length is $a_{\text{sl}} = R[1 - \tan \alpha_0(R-c)/\alpha_0 R]$ and the effective range is r_0 (see Table I for values). The effective range r_0 and derivative $\partial \delta_0/\partial k$ are

$$r_0 = R - \frac{1}{\alpha_0^2 a_{\text{sl}}} - \frac{1}{3}\frac{R^3}{a_{\text{sl}}^2} + c\left(1 - \frac{2R}{a_{\text{sl}}} + \frac{R^2}{a_{\text{sl}}^2} + \frac{1}{\alpha_0^2 a_{\text{sl}}^2}\right),$$
$$\frac{d\delta_0}{dk} = -\frac{a_{\text{sl}}}{1 + a_{\text{sl}}(a_{\text{sl}} - r_0)k^2 + \frac{1}{4}(r_0 a_{\text{sl}})^2 k^4}\left(1 + \frac{r_0 a_{\text{sl}}}{2}k^2\right). \tag{6}$$

When the k^4 term in Eq. (6) is neglected, the integral B_C can be done analytically:

$$B_C \equiv Z \frac{1}{\pi} \int_0^\infty \frac{d\delta_0}{dk} \exp(-bk^2) dk$$
$$= -\frac{a_{\text{sl}}^2(2a_{\text{sl}} - 3r_0)}{4(a_{\text{sl}}^2 - a_{\text{sl}} r_0)^{3/2}} \exp\left(\frac{b}{a_{\text{sl}}^2 - a_{\text{sl}} r_0}\right)$$
$$\times \text{erfc}\left[\sqrt{b/(a_{\text{sl}}^2 - a_{\text{sl}} r_0)}\right] - \frac{a_{\text{sl}}^2 r_0}{4(a_{\text{sl}}^2 - a_{\text{sl}} r_0)\sqrt{\pi b}}. \tag{7}$$

Here $b = \hbar^2/2\mu k_B T = \lambda_T^2(\mu)/2\pi$ and $\text{erfc}(\sqrt{b/a_{\text{sl}}^2}) = 1 - \text{erf}(\sqrt{b/a_{\text{sl}}^2})$. The Boltzmann exponential factor $\exp(-bk^2)$ suppresses the k^4 term in $\partial \delta_0/\partial k$ and makes Eq. (7) a very good approximation to the complete effective range result. This is true even at high energies, as shown in Fig. 1 where calculations of B_C using a square well δ_0 and an effective range approximation are shown.

As previously noted, at high temperatures P and higher order partial waves also contribute. The P-wave phase shift for a square-well potential in the absence of a hard core is
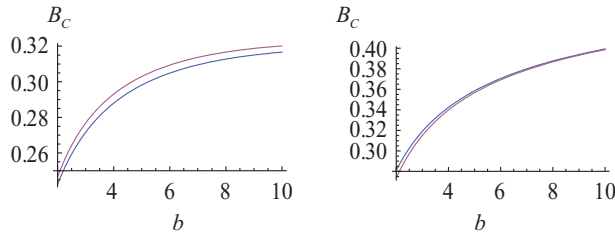
FIG. 1. (Color online) The quantity B_C vs the parameter b. (Left) The upper curve is the approximate analytic expression of Eq. (7); the lower curve is the square-well result using the *nn* parameters of Table I. (Right) The lower curve is the unitary limit of Eq. (7) ($a_{sl} \rightarrow \infty$). The upper curve is the exact square well in the unitary limit with the well depth adjusted to give a zero-energy resonance. For this comparison, the effective range in Eq. (7) was taken to be the same as the square well, $r_0 = R + c = 2.27$. In both panels the error is less than a few percent over a very large range of temperatures and corresponding energy. For $k_B T = 40$ MeV, $b \approx 1$, and for $k_B T = 4$ MeV, $b \approx 10$. The effective range approximation result is very close to the exact square-well result even at high energy or temperature because of the Boltzmann factor.

given by

$$\tan \delta_1 = \frac{Rk\alpha^2 \tan \alpha R - Rk^2\alpha \tan kR - \alpha_0^2 \tan kR \tan \alpha R}{Rk^2\alpha + \alpha_0^2 \tan \alpha R + Rk\alpha^2 \tan kR \tan \alpha R}.$$

(8)

The extension to a square well with a hard core leads to a more complicated expression. The following features of higher l values can be noted. The angular momentum P waves start to become important when the angular momentum barrier $l(l + 1)\hbar^2/2\mu R^2$ is ~ 15 MeV. At higher $T (k_B T \sim 40$ MeV) the S, P, and D waves have contributions to the continuum partition function $z_c \equiv (2J + 1)(2I + 1)/\pi \int (\partial \delta_{JT}/\partial k) \exp(-\hbar^2 k^2/2\mu k_B T) dk$ as follows. The values are $z_c = -1.66, 0.2$ for $^3S_1, ^1S_0; 0.4, -0.12, 0.14, -0.12$ for $^3P_0, ^3P_1, ^3P_2, ^1P_1$; and $0.05, 0.05, -0.15, +0.23$ for $^1D_2, ^3D_3, ^3D_1, ^3D_2$, respectively. $^3S_1$ dominates with -1.66; see Ref. [15], which gives an early application of the Beth-Uhlenbeck expression to nuclear heavy-ion physics. A recent detailed study of the role of higher partial waves in the second virial coefficient for pure neutron matter ($y = 0$) can also be found in Horowitz and Schwenk [17]. Higher partial waves start to become important above 15 MeV, as can be seen in Fig. 1 of Ref. [17]. Further details of the contribution of higher partial waves in the present work will be given in a future study.

The limit $a_{sl} \rightarrow \infty$ is called the universal thermodynamic or unitary limit. In this limit the scattering length no longer appears in expressions such as the energy, but the energy is also no longer an ideal Fermi gas result. The quantity $\Delta B_C \equiv -B_C - (2/3)b\partial B_C/\partial b$ appears in ε_{int} and $\hat{\varepsilon}_{int}$. In the limit of large scattering length a_{sl} and infinite scattering length, the quantity ΔB_C has the following behavior:

$$\Delta B_C \rightarrow \frac{1}{6} \frac{r_0}{\sqrt{\pi b}} \left[1 + \frac{r_0}{a_{sl}} + \left(\frac{r_0}{a_{sl}}\right)^2 \right]$$

$$+ \text{sign}(a_{sl}) \left[\frac{1}{2} - \frac{4}{3\sqrt{\pi}} \frac{\sqrt{b}}{a_{sl}} \left(1 + \frac{r_0}{2a_{sl}}\right) \right.$$

$$\left. + \frac{5}{6} \frac{b}{a_{sl}^2} - \frac{3}{16} \left(\frac{r_0}{a_{sl}}\right)^2 \right], \tag{9}$$

$$\Delta B_C(a_{sl} \rightarrow \infty) \rightarrow \text{sign}(a_{sl}) \left(\frac{1}{2}\right) + \frac{1}{6} \frac{r_0}{\sqrt{\pi b}}$$

$$= \text{sign}(a_{sl}) \left(\frac{1}{2}\right) + \frac{1}{6} \sqrt{2} \frac{r_0}{\lambda_T}.$$

The factor r_o/λ_T appears as a correction to the universal thermodynamic limit of sign$[a_{sl}]/2$. By comparison, for $b/(a_{sl}^2 - a_{sl}r_0) \gg 1$, $B_C \rightarrow -a_{sl}/2\sqrt{\pi b}$, $\Delta B_C = -2B_C/3$. The unscaled interaction density is $\varepsilon_{int} = a_{sl}(\pi\hbar^2/m)(A/V)^2$ when $\Delta B_C = -2B_C/3$. This form of the unscaled interaction density is realized in atomic systems by tuning away from the Feshbach resonance [7]. The value of ΔB_C using phase shifts calculated with a square-well/hard-core potential also closely approximates the results from Eq. (9). When the scattering length a_{sl} becomes infinite, the effective range r_0 goes to $R + c$. A bound state has $-B_b + (2/3) T \partial B_b/\partial T = -\exp[E_b/k_B T] [1 + (2/3) E_b/k_B T] \rightarrow -1$ in the unitary limit of $E_b \rightarrow 0$. Thus, in this limit, a bound deuteron has $a_{sl} \rightarrow +\infty$ and a contribution $-1 + \Delta B_C(a_{sl} \rightarrow \infty) = -1 + (1/2) + r_0/6 (\pi b)^{1/2} = -1/2 + r_0/6(\pi b)^{1/2} = \Delta B_C(a_{sl} \rightarrow -\infty)$, that is, the same contribution for an unbound state where $a_{sl} \rightarrow -\infty$, assuming that the effective range r_0 is the same. The second virial coefficient becomes

$$\frac{\hat{b}_2}{\lambda_T^3} = \left[-\frac{1}{2^{7/2}} + \frac{1}{2^{3/2}} - \frac{2^{3/2}}{4} \left(\frac{1}{4\sqrt{\pi}} \frac{r_{0s}}{\sqrt{b}}\right) \right]$$

$$+ y(1 - y) \left[\frac{5}{2^{5/2}} + \frac{2^{3/2}}{4} \left(\frac{1}{4\sqrt{\pi}} \frac{r_{0s} - 3r_{0t}}{\sqrt{b}}\right) \right]. \tag{10}$$

Here $\hat{b}_2$ includes exchange correlations from antisymmetrization and the formula is for an isospin-symmetric case with all nn, pp, and np singlet effective ranges ($\equiv r_{0s}$) taken to be the same. r_{0t} is the np triplet effective range. Figure 2 shows plots of $\hat{b}_2/\lambda_T^3$ versus y in the universal thermodynamic limit and compares it to $\hat{b}_2/\lambda_T^3$ using the effective range
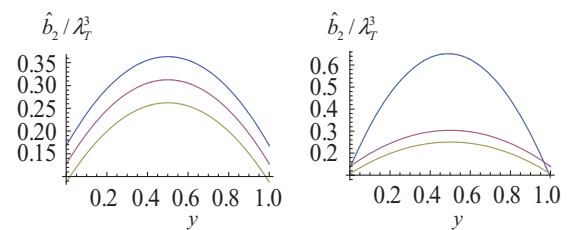

FIG. 2. (Color online) $\hat{b}_2/\lambda_T^3$ vs y. The left figure is the behavior of $\hat{b}_2/\lambda_T^3$ with y for an isospin-symmetric case in the universal thermodynamic limit obtained from Eq. (10). The spread in the three unitary limit curves comes from $r_0/\sqrt{b} \sim r_0/\lambda_T$ terms, which are present even in the unitary limit. A triplet $r_{0t} = 1.75$ fm and singlet $r_{0s} = 2.56$ fm (average of *nn* and *np*) were used. The three curves are for $k_B T = 6, 12$, and 20 MeV with higher curves corresponding to lower $k_B T$. The right figure uses the effective range parameters of Table I and also includes a bound deuteron state. The same three $k_B T$ values are used with the higher curves having lower $k_B T$. At high temperatures the deuteron contribution is considerably reduced.

TABLE I. Experimental values of a_{sl} and r_0 [25] followed by square-well parameters and calculated values. A value of $c = 0.27$ fm was used throughout. The np $S = 1$ parameters bind the deuteron at 2.2 MeV. The pp system has Coulomb terms with $a_{sl} = -7.821$ fm, $r_{0s} = 2.83$ fm. The units of $a_{sl} r_0$, and R are given in femtometers with V_0 in MeV. More recent values of a_{sl} and r_0 can be found in Ref. [26]. The results given in this paper are insensitive to the precise values of these quantities, which are similar in Refs. [25] and [26].

	np $S = 1$	np $S = 0$	nn $S = 0$
Exp	$a_{sl} = a_t = 5.4$	$a_{sl} = a_{s,np} = -23.7$	$a_{sl} = a_{s,nn} = -17.4$
Exp	$r_0 = r_{0t} = 1.75$	$r_0 = r_{0s,np} = 2.73$	$r_0 = r_{0s,nn} = 2.4$
$\{V_0, R\}$	$\{57.14, 1.8\}$	$\{23.18, 2.3\}$	$\{31.60, 2.0\}$
Cal	$a_{sl} = a_t = 5.4$	$a_{sl} = a_{s,np} = -23.70$	$a_{sl} = a_{s,nn} = -17.4$
Cal	$r_0 = r_{0t} = 1.73$	$r_0 = r_{0s,np} = 2.69$	$r_0 = r_{0s,nn} = 2.40$

and scattering length parameters of Table I. The EOS is $PV/Ak_BT = 1 - (\hat{b}_2/\lambda_T^3) \cdot (A/V) \cdot \lambda_T^3$.

The importance of the bound state can be seen in the height in the curves on the left compared to those on the right.

In the limiting cases of the square-well plus hard-core model, one has the following:

(i) A one-component uncharged Fermi gas is obtained by setting $y = 0$.

(ii) A purely attractive square well is obtained by setting $c = 0$ for the core radius.

(iii) A hard-sphere gas is obtained by taking the limit $R \rightarrow c$ and $V_0 \rightarrow 0$. Then $\delta_0 = -kc$ and $d\delta_0/dk = -c$ and, in general, $\tan\delta_l = j_l(kc)/\eta_l(kc)$. P waves have $\delta_1 = -kc + \arctan(kc)$ and D waves have $\delta_1 = -kc + \arctan[3kc/(3 - (kc)^2)]$.

(iv) A Bose gas has a $+$ sign of the exchange term from symmetrization, that is, $x_k = (\pm 1)^{k+1}/k^{5/2})(V/\lambda_T^3)$ with $+$ for bosons and $-$ for fermions.

The term $\hat{b}_2/\lambda_T^3$ can be compared with a spinless hard-sphere Bose gas (from $l = 0$) [23] and a "spinless" hard-sphere Fermi gas (from $l = 1$ only since it is spinless in Ref. [24]) having, respectively, $\hat{b}_2/\lambda_T^3 = (1/2^{5/2} + 2c/\lambda_T)$ and $\hat{b}_2/\lambda_T^3 = [-1/2^{5/2} + 6\pi(c/\lambda_T)^3]$. The P-wave Fermi gas is a limit of large λ_T/c. A system of protons and neutrons has terms that arise from fermions of the same type (pp and nn) coupled to $S = 0$ for $l = 0$ and fermions that are different (np), which can couple to both $S = 0$ and 1. Note that the range of the force to thermal wavelength appears in these results, which bears a similarity to the effective range to thermal wavelength result in the universal thermodynamic limit developed here. Higher angular momentum appear as $(c/\lambda_T)^{2l+1}$.

The rescaled $\hat{\varepsilon}_{int}$ versus y in the unitary limit with one singlet and one triplet effective range is simply

$$\hat{\varepsilon}_{int} = \left[-\frac{1}{2} + \left(\frac{1}{6\sqrt{\pi}} \frac{r_{0s}}{\sqrt{b}} \right) \right]$$
$$+ y(1-y) \left[-1 + \left(\frac{1}{6\sqrt{\pi}} \frac{3r_{0t} - r_{0s}}{\sqrt{b}} \right) \right]. \quad (11)$$

The $r_0/\sqrt{b} \sim r_0/\lambda_T$ part of the rescaled $\hat{\varepsilon}_{int}$ leads to a T-independent $\varepsilon_{int} \sim T\lambda_T^3 \hat{\varepsilon}_{int} \sim r_0$ part. Properties of $\hat{\varepsilon}_{int}$ versus y are shown in Fig. 3.

Higher order cluster terms in a virial expansion become important when the d concentration is large enough to produce further reactions such as the formation of α particles from $d + d \Leftrightarrow \alpha$ or $n + d \Leftrightarrow t$ for tritons [15,16]. The Saha equation gives $N(_ZA_N)/N(p)^Z N(n)^N = (\lambda_T^3/V)^{A-1}(A^{3/2}/2^A)Z_{int}(_ZA_N)$ for the number of clusters with (Z, N). The ratio of ground-state α particles to deuterons d is $N(\alpha_{gs})/N(d) = [N(p) \lambda_T^3/V][N(n)\lambda_T^3/V](\sqrt{2}/6)\exp\{[E_b(\alpha) - E_b(d)]/k_BT\} = [N(d)\lambda_T^3/V](1/9)\exp\{[E_b(\alpha) - 2E_b(d)]/k_BT\}$. The cluster yields decrease rapidly with A when the nucleon density ρ_N and λ_T^3 satisfy $(\rho_N\lambda_T^3/4)\exp(e_b/k_BT) \ll 1$ for $y = 1/2$, where e_b is the binding energy per particle. Moreover, a signal for the presence of very large clusters is the formation of the liquid-gas phase transition, which occurs at $k_BT \sim 9$ MeV for $\rho_N \equiv \rho_{LG} \sim 0.075$ nucleons/fm^3. At temperatures $k_BT \approx e_b = 8$ MeV, the Boltzmann factor in binding energy plays an important role. In fact, because of the large binding effect of the α particle compared to the deuteron $[E_b(\alpha) - 2E_b(d) \approx 24$ MeV], the α particle can dominate at low T [16] because of the Boltzmann factor in binding energy. The proton fraction y also plays a significant role in systems with small y since $N(_ZA_{N(1-y)}) \sim y^Z(1 - y)^N$. Thus an α particle will be more suppressed compared to a deuteron when $y \approx 0$ since $N(\alpha) \sim y^2$, $N(d) \sim y$. Very small y are present in a neutron star [27]. Low concentrations of proton and electrons are necessary to
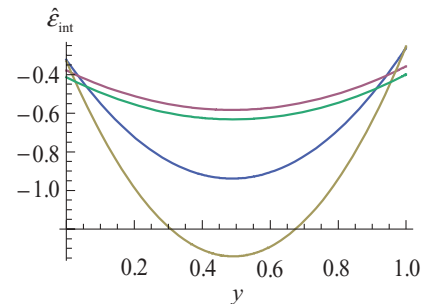

FIG. 3. (Color online) $\hat{\varepsilon}_{int}$ in MeV vs y for various T. The lowest two curves are obtained from the scattering parameters of Table I and contain the deuteron bound state. The two curves correspond to $k_BT = 6$ and 12 MeV. Deeper curves have lower k_BT. The upper flatter curves are the universal thermodynamic limits. These curves are obtained by setting the scattering lengths equal to infinity and the deuteron binding energy equal to zero.

Pauli block neutron β decay. The equilibrium is reached through $n \rightarrow p + e^- + \bar{\nu}_e$ and $p + e^- \rightarrow n + \nu_e$ with the neutrinos escaping. Another higher order consideration is symmetrization effects of even-A bosonic clusters and antisymmetrization effects of odd-A fermionic clusters. Higher order virial coefficients have a complicated structure, as can be seen in the expansion of the EOS in terms of the x'_k values just given. Features associated with the third virial coefficient and its complexity and difficulties are discussed in Ref. [28]. Moreover, large cancellations can occur and it is not clear how to handle the continuum of higher order terms such as the fourth coefficient. A large cancellation is especially true for the virial expansion of a one-component Fermi gas with only antisymmetrization effects included. The EOS, with $x_k = (-1)^{k+1}(1/k^{5/2})V/\lambda_T^3$ and spin degeneracy g_S, reads $P/k_B T = \rho[1 + 0.1766(\rho\lambda_T^3/g_S) - (3.3 \times 10^{-3})(\rho\lambda_T^3/g_S)^2 + (1.11 \times 10^{-4})(\rho\lambda_T^3/g_S)^4]$. The numerical coefficients decrease by $\sim 1/30$. Bound-state cluster contributions are reduced by the continuum correlations from the Levinson theorem: $\delta_l(0) - \delta_l(\infty) = N_l\pi$, where N_l is the number of bound states. In particular, the deuteron contribution is reduced by the $^3S_1$ decreasing phase shift, which starts at π since $N_{l=0} = 1$. The ratio $|B_C(np, 1)|/B_b(np, 1)$ for the continuum to bound contributions in Eq. (5) is 0.28, 0.42, 0.52, and 0.69 for $k_B T = 6, 12, 20,$ and 40 MeV, respectively. Since the phase shift $^3S_1$ in the np $S = 1$ channel is a decreasing function of k, the value of B_C of Eq. (7) is negative.

A finite-temperature two-component model of strongly correlated protons and neutrons, each with two spin states and underlying isospin symmetries, was discussed. The model is an extension of the one-component two-spin-state fermionic models in both atomic systems and in nuclear physics where pure neutron systems are considered. Features associated with Feshbach resonances and bound states can be studied by tuning on the proton fraction y and varying the temperature T. In atomic systems the tuning is done in a controlled way by a magnetic field, which can change the scattering length across

infinity with associated divergences of the size of the resonant state. In the nuclear case the bound state is the spin $S = 1$, isospin $I = 0$ state of the np system, the deuteron, which is loosely bound. Resonant-like virtual structures arise in the $S = 0$, $I = 1$ channels. The nn and np $S = 0$, $I = 1$ channels have very large scattering lengths and approximate the infinite limit. The mixture with varied neutron/proton asymmetry has both positive and negative scattering lengths and is therefore different from the one-component atomic case tuned by the magnetic field. When the scattering lengths a_{sl} are large compared to interparticle spacings and range of interparticle forces, a regime called the unitary limit is reached and this limit was studied and compared to calculations using experimental values for a_{sl} and r_0. A simplified interaction between nucleons was used: an attractive square-well potential with a short-range hard-core repulsion. Properties of this potential were then related to experimental results for nucleon-nucleon effective ranges r_0 and a_{sl} in spin singlet and triplet states. Analytic results were developed in an effective range approximation for various features such as the interaction energy and EOS. A rescaled interaction energy $\hat{\varepsilon}_{int}$ was shown to be relatively flat with variation with y in the unitary limit. A variation with T in $\hat{\varepsilon}_{int}$ comes from a residual dependence on the ratio r_0/λ_T that appears in the results even in the limit of infinite scattering length. The associated ε_{int} is T independent. The deuteron bound state was shown to produce a large departure in the interaction energy from the unitary limit and give rise to a pronounced T dependence at low T. Higher order clusters are also important, and in particular the α particle can dominate [16] in a virial expansion. Another extreme of large λ_T/a_{sl} was also studied. In atomic systems this other limit is realized by tuning away from the Feshbach resonance. Comparisons were also made with hard-sphere Bose and Fermi gases, which are limiting cases of the potential used.

[1] G. F. Bertsch, Int. J. Mod. Phys. B **15**, iii (2001).
[2] K. M. O'Hara *et al.*, Science **298**, 2179 (2002).
[3] T. Bourdel *et al.*, Phys. Rev. Lett. **91**, 020402 (2003).
[4] K. Dieckmann *et al.*, Phys. Rev. Lett. **89**, 203201 (2002).
[5] C. A. Regal *et al.*, Nature (London) **424**, 47 (2003).
[6] T.-L. Ho, Phys. Rev. Lett. **92**, 090402 (2004).
[7] T-L. Ho and E. Mueller, Phys. Rev. Lett. **92**, 160404 (2004).
[8] J. Carlson, S.-Y. Chang, V. R. Pandharipande, and K. E. Schmidt, Phys. Rev. Lett. **91**, 050401 (2003).
[9] A. Bulgac, J. Drut, and P. Magierski, Phys. Rev. Lett. **99**, 120401 (2007).
[10] A. Schwenk and C. J. Pethick, Phys. Rev. Lett. **95**, 160401 (2005).
[11] G. A. Baker, Phys. Rev. C **60**, 054311 (1999).
[12] H. Heiselberg, Phys. Rev. A **63**, 043606 (2001).
[13] D. Dean and T. Schafer, Phys. Rev. C **72**, 024006 (2005).
[14] H.-M. Mueller, S. E. Koonin, R. Seki, and U. van Kolck, Phys. Rev. C **61**, 044320 (2000).
[15] C. J. Pethick and D. G. Ravenhall, Annu. Rev. Nucl. Part. Sci. **45**, 429 (1995).
[16] A. Z. Mekjian, Phys. Rev. C **17**, 1051 (1978).
[17] C. J. Horowitz and A. Schwenk, Nucl. Phys. **A776**, 55 (2006).
[18] C. J. Horowitz and A. Schwenk, Phys. Lett. **B638**, 153 (2006); **B642**, 326 (2006).
[19] S. Pratt, P. Siemens, and Q. N. Usmani, Phys. Lett. **B189**, 1 (1987).
[20] K. C. Chase and A. Z. Mekjian, Phys. Rev. C **50**, 2078 (1994).
[21] C. Das, S. Das Gupta, W. Lynch, A. Mekjian, and B. Tsang, Phys. Rep. **406**, 1 (2005).
[22] S. Das Gupta and A. Z. Mekjian, Phys. Rev. C **57**, 1361 (1998).
[23] E. Beth and G. E. Uhlenbeck, Physica **4**, 915 (1937).
[24] K. Huang, *Statistical Mechanics* (Wiley, New York, 1987).
[25] R. K. Pathria, *Statistical Mechanics* (Pergamon, New York, 1972).
[26] M. A. Preston and R. K. Bhaduri, *Structure of the Nucleus* (Addison Wesley, Reading. MA, 1975).
[27] A. Gardestig, J. Phys. G **36**, 053001 (2009).
[28] S. Weinberg, *Gravitation and Cosmology* (Wiley, New York, 1971).
[29] P. F. Bedaque and G. Rupak, Phys. Rev. B **67**, 174513 (2003).